Proton Dynamics in the Strong Chelate Hydrogen Bond of Crystalline Picolinic Acid *N*-Oxide. A New Computational Approach and Infrared, Raman and INS Study

Jernej Stare,*,†,‡ Jarosław Panek,§ Juergen Eckert,‡,|| Jože Grdadolnik,† Janez Mavri,† and Dušan Hadži*,†

National Institute of Chemistry, Ljubljana, Slovenia; Center for Non-Linear Studies/Los Alamos Neutron Science Center, Los Alamos National Laboratory, Los Alamos, New Mexico; Faculty of Chemistry, Wrocław University, Wrocław, Poland; and Materials Research Laboratory, University of California, Santa Barbara, California

Received: September 4, 2007; In Final Form: November 26, 2007

Infrared, Raman and INS spectra of picolinic acid *N*-oxide (PANO) were recorded and examined for the location of the hydronic modes, particularly O−H stretching and COH bending. PANO is representative of strong chelate hydrogen bonds (H-bonds) with its short O···O distance (2.425 Å). H-bonding is possibly well-characterized by diffraction, NMR and NQR data and calculated potential energy functions. The analysis of the spectra is assisted by DFT frequency calculations both in the gas phase and in the solid state. The Car−Parrinello quantum mechanical solid-state method is also used for the proton dynamics simulation; it shows the hydron to be located about 99% of time in the energy minimum near the carboxylic oxygen; jumps to the N−O acceptor are rare. The infrared spectrum excels by an extended absorption (Zundel's continuum) interrupted by numerous Evans transmissions. The model proton potential functions on which the theories of continuum formation are based do not correspond to the experimental and computed characteristics of the hydrogen bond in PANO, therefore a novel approach has been developed; it is based on crystal dynamics driven hydronium potential fluctuation. The envelope of one hundred $0 \rightarrow 1$ OH stretching transitions generated by molecular dynamics simulation exhibits a maximum at 1400 cm^{-1} and a minor hump at ∼1600 cm^{-1}. These positions square well with ones predicted for the COH bending and OH stretching frequencies derived from various one- and two-dimensional model potentials. The coincidences with experimental features have to be considered with caution because the CPMD transition envelope is based solely on the OH stretching coordinate while the observed infrared bands correspond to heavily mixed modes as was previously shown by the normal coordinate analysis of the IR spectrum of argon matrix isolated PANO, the present CPMD frequency calculation and the empirical analysis of spectra. The experimental infrared spectra show some unusual characteristics such as large temperature effects on the intensity of some bands, thus presenting a challenge for theoretical band shape treatments. Our calculations clearly show that the present system is characterized by an asymmetric single well potential with no large amplitudes in the hydronium motion, which extends the existence of Zundel-type spectra beyond the established set of hydrogen bonds with large hydronic vibrational amplitudes.

1. Introduction

The understanding of the infrared (IR) spectra and proton dynamics of molecules with chelate type intramolecular hydrogen bonds of moderately short O···O distances ($d_{O\cdots O} < 2.6$ Å) has progressed to the point of good agreement between experimental and computed band frequencies and shapes. Benchmark examples are malonaldehyde and acetylacetone. The OH_s mode (see Abbreviations at the end of the Introduction) is unequivocally located in their IR spectra; its positions and band shapes are convincingly reproduced by calculations.[1−11] However, the situation concerning molecules with stronger intramolecular H-bonds is much less satisfactory.

Difficulties in locating vibrational modes with major contributions of OH_s and COH_{be} internal coordinates are rising with decreasing $d_{O\cdots O}$ below 2.48 Å. On the experimental side, it is the broadness and low peak intensity of the absorption appearing in the region above 1800 cm^{-1} of the IR spectra of, e.g., enolones or, even worse, below this limit. This can lead to complete failure in observing such absorption, e.g., in hydroxyphenalenone[12] and naphthazarin,[13] or to controversies in the interpretation of their origin if eventually observed. For example, in the IR spectra of dibenzoylmethane and its congeners, a weak and broad absorption culminating between 2600 cm^{-1} and 1800 cm^{-1} is ubiquitous. It is usually attributed to the OH_s fundamental,[14,15] but Emsley and co-workers[16,17] attribute this absorption to combination modes and/or higher order transitions while predicting the OH_s fundamental to be near 1550 cm^{-1}. Controversies in the interpretation of spectra and dynamics exist even in the benchmark example of very short $d_{O\cdots O}$ which is hydrogen maleate.[18,19]

Ab initio and DFT calculations at the harmonic level are inadequate in the quest for the OH_s mode since anharmonicity and the red shift of this mode increase with the shortening of

* To whom correspondence should be addressed. E-mail: jernej@cmm.ki.si, dusan.hadzi@ki.si.
† National Institute of Chemistry.
‡ Los Alamos National Laboratory.
§ Wrocław University.
|| University of California.

10.1021/jp077107u CCC: $40.75
Published on Web 01/29/2008

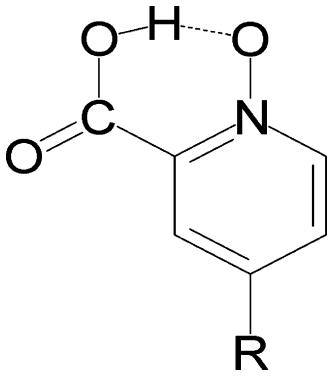

Figure 1. Picolinic acid *N*-oxide (PANO) (R = H). Among the congeners mentioned in this paper is 4-nitro PANO (R = NO_2).

$d_{O\cdots O}$.[20] The discrepancies between the OH_s frequencies calculated at the harmonic level and the experimental ones are less spectacular in examples with longer $d_{O\cdots O}$,[21,22] but they are rapidly increasing with the shortening of $d_{O\cdots O}$ and concomitant shifting of the OH_s frequencies into the range of skeletal modes and coupling therewith. Even the use of the anharmonic analysis implemented in *Gaussian 03* program package that includes anharmonicity at the level of quartic potentials did not yield acceptable results in the example of picolinic acid *N*-oxide (PANO, Figure 1) isolated in argon matrix.[23]

The experimental and computational hurdles experienced with molecules in matrix or solution increase when turning to crystal phase spectra. The spectra of PANO are an outstanding example of differences between the spectra of various phases. On the experimental side, an additional source of difficulties in the interpretation of the crystal phase spectra arises from the appearance of the extended absorption, also known as Zundel continuum,[24] with Evans transmissions.[25,26] On the computational side, the extensive coupling of the hydronic[27] coordinates with the skeletal ones and the effects of crystal dynamics require the accounting of periodicity.

In order to contribute to the clarification of these problems and to test the available methods we have investigated the IR, Raman and INS spectra of PANO and some of its substituted congeners.[28] Advantages of this series lie in the chemical homogeneity, the absence of possible steric compression leading to a shortening of $d_{O\cdots O}$ other than from electronic effects, and the absence of proton tunneling. The range of $d_{O\cdots O}$ covered by the series (2.48 Å to 2.40 Å) permits a systematic pursuit of the effects of increasing the H-bond strength on the evolution of vibrational spectra and other physical characteristics. In this article use of this study will be made occasionally; the details will be published separately.

The IR spectra of PANO and its congeners in the solid and in solution phases have been investigated earlier.[29−32] However, some important points were not considered or were misinterpreted. Infrared solution spectra, one-dimensional potentials and OH_s frequencies of PANO and some representative derivatives have been also published;[33] spectra of solids were shown in that article only to expound the large differences between the spectra of solutions and solids that are indicative of the sensitivity of the potential hypersurface to the effect of surroundings.

In this paper we shall concentrate on the IR, Raman and INS spectra of the unsubstituted compound. One reason for this lies in the availability of a substantial amount of information on its H-bond characteristics obtained by other methods (see preamble of the Results and Discussion section) which ranks PANO among the best characterized examples of chelate H-bonds with short $d_{O\cdots O}$. The main reason lies, however, in the recent study[23] of the IR spectra of matrix isolated PANO that includes the quantum-mechanics-based normal coordinate analysis (NCA). The very good agreement between the calculated and experimental frequencies and intensities obtained in this work offers a useful guide to the interpretation of the crystal spectra, particularly in exposing the mixed character of the modes sought for. However, the strength of the interactions between the molecules and the dynamic effects of the lattice modify the molecular potential hypersurface and thereby alter the frequencies and intensities with respect to the isolated molecule.[34] A separate investigation of the crystal phase appears attractive; therefore we carried out the periodic Car−Parrinello frequency calculations at the harmonic level as a first choice. In the CPMD simulation the crystal field effects on the molecular structure are properly considered, while the dynamics of the nuclei is still classical. The frequencies of some protonic modes, particularly OH_s, calculated in the harmonic approximation are, however, in poor agreement with the experimental IR spectra in contrast to ones involving the ring modes. This is not surprising in view of the effect of anharmonicity evident in the NCA[23] and in frequencies calculated from proton potentials. However, the calculated CPMD frequencies are in overall good agreement with the observed INS spectra. This is also true of the INS intensities produced by the methodology built in the CLIMAX program[35,36] from the amplitudes given by the CPMD calculation. Unfortunately, the CPMD calculated frequency of the mode with dominant OH_s internal coordinate is neither in agreement with ones resulting from reliable potential surface calculations nor in agreement with the results of the NCA study,[23] nor is it observable in the experimental spectra. Moreover, crystal field effects produce large temperature dependence of some bands that seems to be unique and thus challenging for theoretical studies.

The failure to identify well-defined candidates for the hydronic stretching modes either from the CPMD calculation or in the INS spectra dictated a thorough empirical analysis including Raman spectra and the spectra of the ^2H and ^{18}O isotopomers. Although this exercise brought to light a candidate for the internal coordinate involving largely the coupled COH_{be} and OH_s motions, no distinct IR band was found, at least at room temperature, that may be attributed to another mode with major OH_s participation. This failure suggested the need of considering the continuum as a hideout for the stretching mode. The extreme broadening of the OH_s mode in the IR spectra of systems with strong H-bonding and large hydronic vibrational amplitudes, also labeled continuum, was extensively elaborated by Zundel and co-workers from both the theoretical and experimental sides (for review see ref 24). However, the present example does not fit well the conditions for exhibiting a continuum as expounded by Zundel,[31] and therefore we developed a novel computational approach. It is based on the solutions of the one-dimensional time-independent vibrational Schrödinger equation for the snapshots extracted from the CPMD simulation. The envelope of the frequency distribution of the $0 \rightarrow 1$ transitions covers a span of some 1000 cm^{-1} with a maximum at about 1400 cm^{-1} thus resembling the observed IR spectra. However, such maximum is not unambiguously identifiable in the observed continuum. In fact, a feature of hydronic character does appear at 1410 cm^{-1} in the IR spectrum, but its narrowness does not permit an unambiguous assignment to the maximum in a frequency distribution.

The article is organized as follows. The experimental and computational sections are followed by a preamble in which the experimental and computed characteristics of the H-bonding

in PANO are collected. This is followed by a commented presentation of the vibrational spectra and the results of the CPMD simulation. The results are summarized in the concluding remarks. Some points requiring further investigations are exposed there.

Abbreviations: IR, infrared; INS, inelastic neutron scattering; CPMD, Car−Parrinello molecular dynamics program suite; NCA, normal coordinate analysis; PED, potential energy distribution; PANO-*h*, PANO-*d*, normal and deuterated PANO, respectively; OH_s, $C{=}O_s$, OH stretching, C═O stretching; COH_{be}, COH in-plane bending, etc.

2. Experimental Section

Infrared and Raman Spectroscopy. Picolinic acid *N*-oxide (PANO) was purchased from Sigma-Aldrich. Different batches of the product contained either α or *β* polymorphs. The desired one was obtained by recrystallization from appropriate solvents. The purity of the samples with respect to morphology was checked by powder diffraction. The deuterated sample is the *β* polymorph irrespective of the solvent (D_2O or CH_3OD) used. Unfortunately, the target 90% deuteration level was not achieved despite the use of all precautions. Mass spectrometric and NMR analysis gave results of 80 ± 5% of deuteration. The IR and Raman spectra were recorded by a Perkin-Elmer 2000 FTIR spectrometer. The GRAMS software was used in manipulating the spectra. The $C{=}^{18}O$ isotopomer was synthesized by Prof. Boris Šket, Faculty of Chemistry and Chemical Technology at the University of Ljubljana.

INS Vibrational Spectroscopy. The INS measurements on samples of PANO and its H-bond deuterated analogue (approximately 1 g each in thin Al containers) were carried out on the crystal-analyzer inverse-geometry spectrometer TOSCA at the ISIS pulsed-neutron source at a temperature of 12 K. The incident neutron beam spans a broad energy (E_0) range, and the energy selection is carried out on the secondary neutron flight-path using the (002) Bragg reflection of a graphite analyzer placed in a backscattering position. The energy resolution of TOSCA is in the range $2\% < (\Delta\hbar\omega/E_0) < 3.5\%$ over the accessible energy transfer range of 24 cm^{-1} to 8065 cm^{-1}.

3. Computational Section

The crystal structure of α-PANO (see below) was modeled according to the X-ray diffraction crystallographic data of Steiner et al.[37] The molecular dynamics simulation was carried out using the Car−Parrinello scheme,[38] as implemented in the CPMD v. 3.7.2 program package.[39] The BLYP density functional coupled with plane-wave basis set with kinetic energy cutoff of 120 Ry and the relativistic Goedecker atomic pseudopotentials[40] were used throughout. The CPMD harmonic frequency calculation was carried out numerically on the basis of finite differences of the built-it analytical energy gradients with respect to nuclear coordinates. Note that CPMD frequency calculation yields only the frequency values and the composition of the corresponding normal coordinates; IR and Raman intensities are, unfortunately, not yet supported by CPMD. The INS vibrational spectrum based on intensities derived from nuclear neutron scattering lengths and their individual vibrational amplitudes was calculated by the CLIMAX[35,36] program with the CPMD harmonic frequencies and normal modes as input. Additionally, anharmonic vibrational analysis, as implemented in the *Gaussian 03* program,[41,42] of the isolated PANO model at the B3LYP/6-31+G(d,p) level of theory at a previously optimized geometry was also carried out. The results of *Gaussian 03* and CPMD geometry optimizations and frequency calculations are listed in Tables 1 and 2. Frequency calculation outputs are also available as Supporting Information (S1a,b).

TABLE 1: PANO Metric Parameters Obtained at Different Levels of Theory

method, model and phase	$d_{O\cdots O}$ [Å]	d_{O-H} [Å]	ref
B3LYP/6-31+G(d,p)/gas-phase monomer	2.509	1.011	*34*
B3LYP/6-31+G(d,p)/gas phase dimer	2.489	1.018	*34*
B3LYP/6-31+G(d,p)/gas phase trimer	2.469	1.027	*34*
B3LYP/6-31+G(d,p)/SCRF (acetonitrile, $\epsilon = 36.6$) monomer	2.464	1.028	*33, 55*
BLYP/PW/crystal	2.457	1.067	*34*
B3LYP/6-31+G(d,p)/gas-phase monomer, averaged geometry over anharmonic vibrational wavefunctions ("freq= anharmonic" keyword in G03)	2.501	1.028	*a*
B3LYP/cc-pVDZ/gas-phase monomer, averaged geometry over anharmonic vibrational wavefunctions ("freq= anharmonic" keyword in G03)	2.509	1.028	*a*
experimental (X-ray diffraction, 125 K)	2.425(2)	1.04(3)	*37*

[a] This work.

The molecular dynamics simulation was carried out at a constant volume (i.e., the unit cell parameters listed above were fixed during the simulation). The fictitious orbital mass was set to 150 au (note that 1 au corresponds to the electron mass), and the propagation time step was set to 2 au (0.048378 fs). The temperature of the system was controlled using the Nosé−Hoover thermostat for the nuclear motion.[43−45] Target temperature and thermostat frequency were set to 300 K and 3200 cm^{-1}, respectively. The structure of PANO was energy minimized prior to the dynamics run. The simulation consisted of about 300 000 steps, i.e., the simulated time was approximately 14.5 ps. The initial period of 2 ps of the dynamics was taken as equilibration and was not further analyzed. Nuclear coordinates were stored to the trajectory file every time step of the simulation.

Snapshots of the dynamics were extracted next from the trajectory every 5000 steps (approximately 242 fs). In such a way 50 distinct snapshot structures as generated by the dynamics simulation were obtained. From each of these structures two proton potential functions (one per PANO molecule in the unit cell) were acquired by stepwise displacing the H-bonded proton along the O−H bond vector in 0.05 Å steps, covering the d_{OH} range from 0.75 to 2.00 Å. We demonstrated that proton motion correlation between two adjacent PANO molecules in the unit cell is negligible. Therefore it is not necessary to proceed with two quantum body calculations.[34] A total number of 100 diverse proton potentials (Figure 2a) were obtained in such a way.

Anharmonic vibrational energies and wavefunctions were determined for each of these potentials by solving the vibrational Schrödinger equation. The variational Fourier grid Hamiltonian (FGH) method of Balint-Kurti et al.[46,47] adopted for application in generalized internal coordinates[48] was used for this purpose. A sample potential with corresponding vibrational energy levels and wavefunctions is displayed in Figure 2b. For each of the so obtained $0 \rightarrow 1$ transitions, the relative transition intensity ($I_{0\rightarrow1}$) was calculated according to the formula

TABLE 2: Calculated OH Stretching and COH Bending Frequencies of PANO Using Different Models and Levels of Theory

method, model and phase	OH_s [cm^{-1}]	COH_{be} [cm^{-1}]	ref
harmonic/gas phase (*Gaussian 03*)[a]	2900−3100	1530−1560	*33*
harmonic/solvent (acetonitrile, $\epsilon = 36.6$)[b]	2670	1563	*33, 55*
harmonic/crystal (CPMD)	2158	1530, 1573, 1647[c]	*d*
anharmonic (normal-mode analysis, quartic perturbation)/gas phase[e] B3LYP/6-31+G(d,p)	2363	1501	*d*
anharmonic (normal-mode analysis, quartic perturbation)/gas phase[e] B3LYP/cc-pVDZ	2421	1514	*d*
anharmonic (quantum-mechanics-based normal coordinate analysis)[f]	1867	1743	*23*
anharmonic (1D single point potentials; ν_{OH} or δ_{OH})/gas phase	2638	1543	*34, 55*
anharmonic (1D relaxed potentials; ν_{OH} or δ_{OH})/ gas phase	2100	1528	*34*
anharmonic (2D relaxed potential; ν_{OH}/ν_{OO})/ gas phase	1733	not included	*53*
anharmonic (1D single point potentials; ν_{OH})/crystal	1407	1577	*34, 48*
anharmonic (2D single point potential; ν_{OH}/δ_{OH})/crystal		1767/1299[g]	*48*

[a] Values depend on the level of theory and basis set used. [b] Calculated with the SCRF-PCM approach of Tomasi and coworkers using the B3LYP/6-31+G(d,p) level of theory. [c] Modes with largest COH_{be} contribution (Figure 7a). [d] This work. [e] As implemented in the *Gaussian 03* code using the *"freq=anharmonic"* keyword. A minimized B3LYP/6-31+G(d,p) isolated model was used. [f] Normal coordinate analysis with the O−H stretching force constant scaled to fit the $0 \rightarrow 1$ transition frequency of the one-dimensional relaxed proton potential function. Frequencies of modes with largest PED of respective coordinates are listed. [g] Both fundamental vibrational transitions include comparable contributions of the bending and stretching motion.

$$I_{0\rightarrow 1} = \left(\int \psi_0(x)\cdot\mu(x)\cdot\psi_1(x)\,dx\right)^2$$

where $\psi_0(x)$ and $\psi_1(x)$ are the ground state and the first excited vibrational proton wavefunctions, respectively (note that application of the FGH method yields real rather than complex vibrational wavefunctions), and x is the O−H distance. The dipole moment function, $\mu(x)$, was set to be linear with respect to x (i.e., electrical harmonicity was assumed). The distribution of the resulting vibrational transitions corresponding to the OH_s envelope was plotted against the frequency axis as a set of delta functions. In addition the envelope was approximated by a continuous curve assuming that each individual vibrational transition is a Gaussian function of a constant half-width of 50 cm^{-1} and with its integral being equal to the relative transition intensity defined above. The stretching envelope was also calculated for the deuterated isotopomer of PANO (PANO-*d*) in the same manner as outlined above. The same dynamics trajectory and the same snapshot structures with the corresponding potentials were used; however a different mass corresponding to the isotope change was applied in solving of the vibrational Schrödinger equation by the FGH method. Very recently the same methodology was applied to an intramolecular hydrogen bond of a Mannich base in the gas phase, as well as in solution and in the solid state.[49,50]

In addition to the method outlined above, we tentatively calculated the vibrational power spectrum of solid-state PANO by Fourier transform of the velocity autocorrelation function, obtained from the CPMD simulation. Analysis of the resulting spectrum showed that the main portion of the OH_s mode appears as a broad and very weak absorption located between 2000 and 2500 cm^{-1}. The location of the center of this absorption compares well to the OH_s frequency obtained by harmonic analysis. Interestingly, no red shift due to anharmonicity was observed, suggesting that the sole mechanical anharmonicity of the OH_s potential is not sufficient to bring the mode below 2000 cm^{-1}. This can be explained by the fact that classical molecular dynamics samples the potential energy surface up to 1−2 kcal/mol above its minimum, while with our approach we considered a much larger range of the hydron potential. For instance, zero-point OH_s vibrational levels were about 2.5 kcal/mol (4.5 k_BT) and the first excited levels about 6.7 kcal/mol (11.5 k_BT) above the minimum of the potential. It is therefore necessary to include nuclear quantum effects in the treatment of the hydron dynamics to correctly account for the enormous red shift of the OH_s mode. Apart from the main OH_s absorption in the vibrational power spectrum, small contributions of the OH_s coordinate can be observed at just above 1500 and 1000 cm^{-1}, suggesting small couplings of the in-plane and out-of-plane COH_{be} modes to the OH_s. However, these couplings are probably quite different in their nature and much less pronounced than the observed ones, mainly because of the significantly overestimated range of the OH_s frequency. In addition, due to compilation problems, we were not able to perform the dipole moment calculation along with the CPMD simulation, hence no reliable IR intensities could be reproduced in the way described above. As the classical nuclear dynamics coupled with the autocorrelation method (particularly in the absence of the time-dependent dipole moment function) does not yield reliable results, it was not further analyzed and discussed.

4. Results and Discussion

Preamble: H-Bond Characteristics. PANO crystals exhibit dimorphism. The monoclinic α form belongs to the $P2_1/m$ space group, $Z = 2$. At 125 K, $d_{O\cdots O}$ is 2.425(2) Å and d_{O-H} is 1.04(3) Å; the OH···O angle is 159°.[37] Interestingly enough, $d_{O\cdots O}$ shortens to 2.418(3) Å at 300 K and the O−H bond extends to 1.18(4) Å.[37] The orthorhombic β form belongs to the P_{mca} space group, $Z = 4$. The molecular geometry in this form is practically the same as in the α form. In both forms the molecules are planar and packed in layers, but the mutual orientation of molecules within the layers is different. The in-plane packing is shown in Figure 3. In the α polymorph, the long axes are parallel, while in β, they form a zigzag pattern with an angle of 20° between the long molecular axes.[51] PANO-*d* was obtained only in the β form. Notable is the discrepancy between the experimental molecular metric parameters and the ones calculated for free molecules. Even if fairly large basis sets are used in geometry optimization, the calculated $d_{O\cdots O}$ are about 0.1 Å too long (Table 1). However, inclusion of the solvent reaction field[52] brings the distance remarkably closer to one obtained in the diffraction studies, and this also is true of $d_{O\cdots O}$ corrected for the quantum effects of the proton motions[33,53] as well as of the structure resulting from the CPMD simulation of the α phase. This gives evidence of the strong effects of polar environment on the structure and dynamics of PANO.

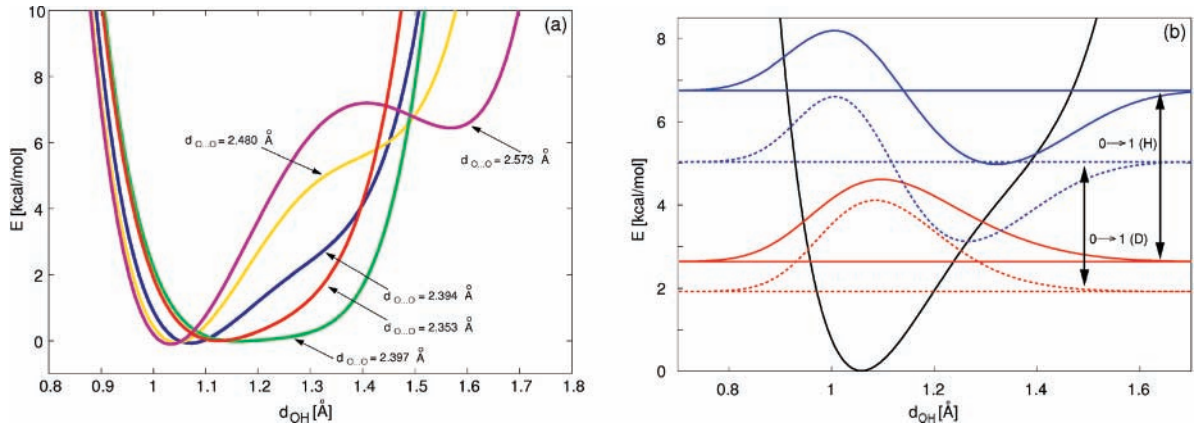

Figure 2. (a) Selected hydron potentials acquired from snapshots of the CPMD simulation of PANO in the solid state together with corresponding snapshot values of the O···O distance. One hundred such potentials were extracted from the simulation presented in this work; for the sake of clarity only five of them are displayed. (b) Sample anharmonic OH_s potential of PANO, corresponding to the fully optimized structure in the solid state ($d_{O\cdots O}$ = 2.457 Å), with the two lowest vibrational levels and wavefunctions (full line, undeuterated; dashed line, deuterated) with the corresponding 0 → 1 transitions indicated.

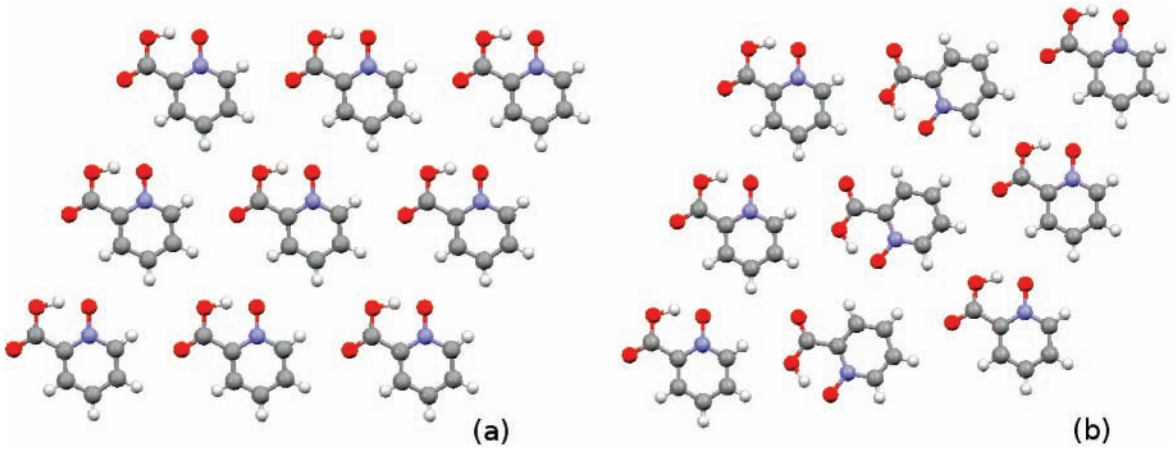

Figure 3. In-plane crystal packing of PANO: (a) in the α polymorph, (b) in the *β* polymorph.

In both the diffraction derived and computed structures the acidic hydrogen is placed clearly next to the carboxylic oxygen. Obviously, this position is determined by an asymmetric potential in agreement with all the calculated ones (see references in Table 1 and 2). A series of potential functions obtained from snapshots of the CPMD simulation is shown in Figure 2a. Note that the shape of the curves does not evolve as a simple function of $d_{O\cdots O}$.

The experimental value of $d_{O\cdots O}$ ranks the H-bond in PANO among the very short, strong ones. The ^{1}H NMR chemical shift of 18.01 ppm in the solid and the deuterium quadrupole coupling constant of 91.1 kHz are in accord with the strength of bonding.[54] The energy of the H-bond calculated as the difference between the chelate structure and the open one with the carboxyl groups rotated by 180° is 14.5 kcal/mol.[55] This value has been corrected for the difference between the *E* and *Z* conformations of the carboxyl group that is about 4 kcal/mol.[56]

Vibrational Spectra. We shall initiate the analysis of the spectra with the unambiguously identifiable features that are the strong bands near 1050 cm^{-1} in the IR and INS spectra (Figures 4a and 6a) and a much weaker feature in the Raman spectra (Figure 5a). They are due to the O−H···O out-of-plane deformation. The deuteration sensitivity and rough accord with the calculated frequencies (Figure 7, S1a, S1b) are supporting the assignment. The same support is offered for the IR bands near 430 cm^{-1} and 291 cm^{-1} (S2a) that are representing the chelate ring deformations with COH_{be} participation (Figure 7a); these modes are counterparts of the O···O stretching in intermolecular H-bonds. The effect of deuteration observed in the INS spectra merits a comment, and we shall consider as example the band at 438 cm^{-1}. It is obviously an unresolved doublet in PANO-*h* giving rise to two bands on deuteration, i.e., 436 cm^{-1} and 405 cm^{-1}. The higher frequency band is due to a chelate ring vibration with a protonic component while the lower frequency band that was unresolved in PANO-*h* moves to 405 cm^{-1} according to the deuteron participation in the respective normal mode; the reduced intensity is in accord with this. The CPMD calculation produces two fairly closely positioned pairs of bands: 433/438 and 457/461 cm^{-1}. The former pair moves to 423/426 cm^{-1} while the second pair remains unaffected. The agreement of the observed and calculated frequencies is acceptable taking into account that the crystal splittings are not resolved and therefore the choice between the available frequencies cannot be made. Similar agreement between INS and harmonic CPMD frequency shifts is observed with the band located at 291 cm^{-1} that moves to 283 cm^{-1} on deuteration. However, the agreement between the experimental and calculated frequencies is of minor importance compared to the agreement between the proposed and calculated shifts. A corresponding explanation can be applied to some higher frequency features.

The identification of bands corresponding to normal modes with major participation of the COH_{be} and OH_s internal coordinate is a far less straightforward task because of the

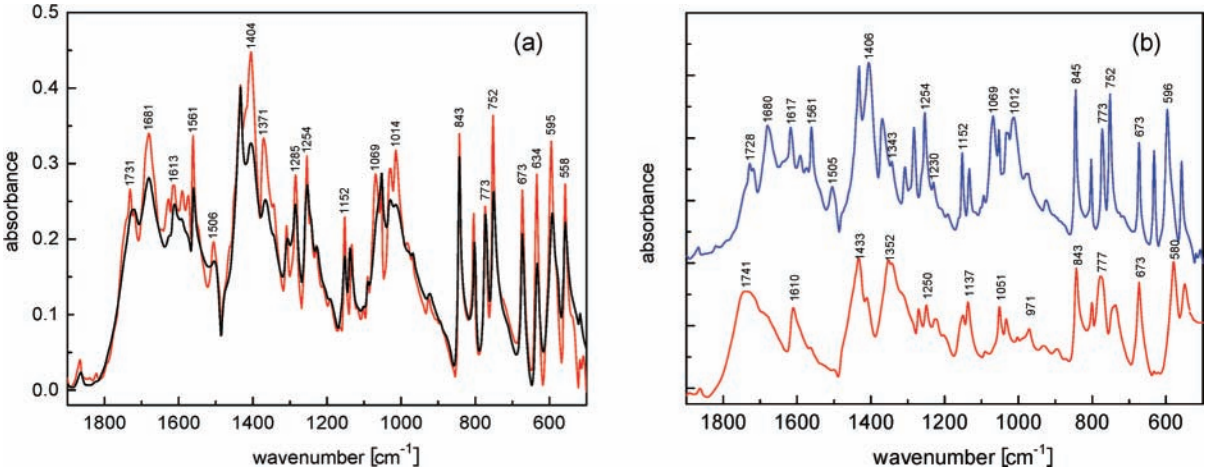

Figure 4. Infrared spectra of picolinic acid *N*-oxide (in KBr pellets): (a) α polymorph (black, 300 K; red, 120 K); (b) *β* polymorph (blue, normal, 120 K; red, deuterated, 300 K).

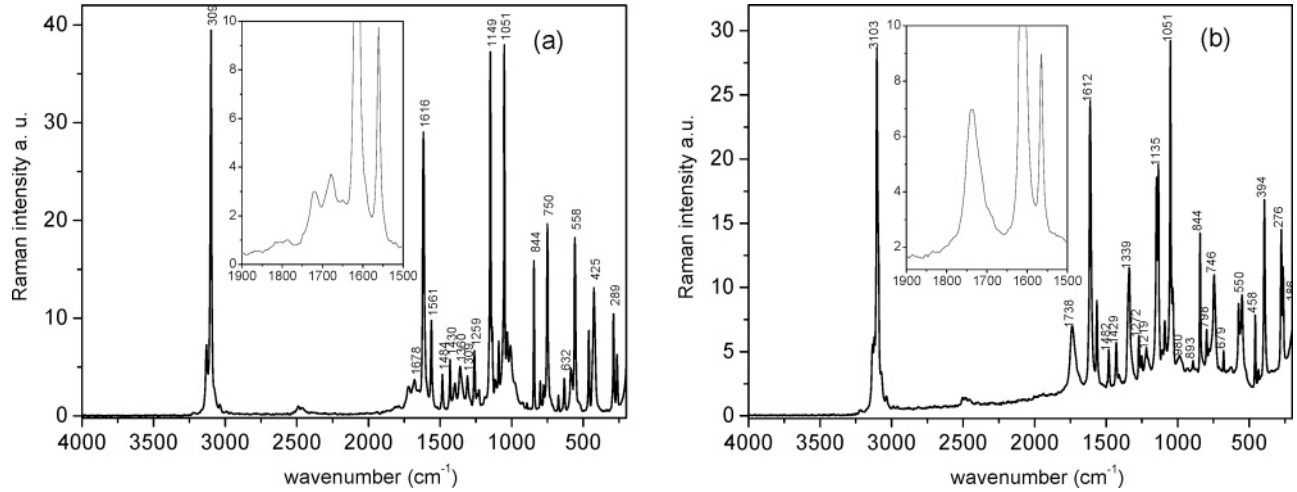

Figure 5. Raman spectra of *β*-picolinic acid *N*-oxide: (a) normal; (b) deuterated. The broad absorption feature is shown in inset.

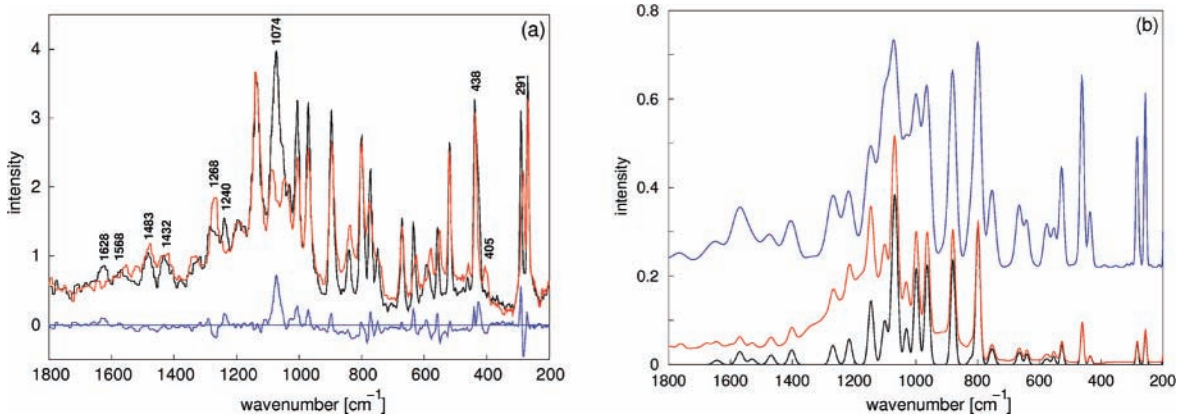

Figure 6. (a) Inelastic neutron scattering spectra of picolinic acid *N*-oxide at 20 K (black, normal; red, deuterated; blue, scaled {H−D} spectral difference). (b) Calculated inelastic neutron scattering spectra from frequencies and amplitudes obtained by CPMD (black, fundamentals only; red, overtones included; blue, overtones and instrumental resolution included).

extensive coupling with C═O_s, C−O_s and N−O_s internal coordinates. Such couplings have been demonstrated by NCA of isolated molecules,[23] and they appear even in the harmonic DFT frequency calculations (S1a,b). Besides those, the anharmonic coupling of the fast OH_s with low-frequency modes of the O−H···O subsystem is expected to contribute to the red shift and band shaping of the OH_s band.[26,57] Fermi resonances also play an important role in the case of IR spectra.

In order to facilitate the location of the COH_{be} modes, we have collected in Table 2 the frequencies predicted by model calculations based on one- and two-dimensional potential functions and on the complete force field calculation. The predicted frequencies of the COH_{be} mode cover a fairly narrow range of ∼100 cm^{-1} irrespectively of the model used, i.e., 1D or 2D potentials or inclusion of all degrees of freedom. According to the CPMD calculation (Figure 7a), the modes

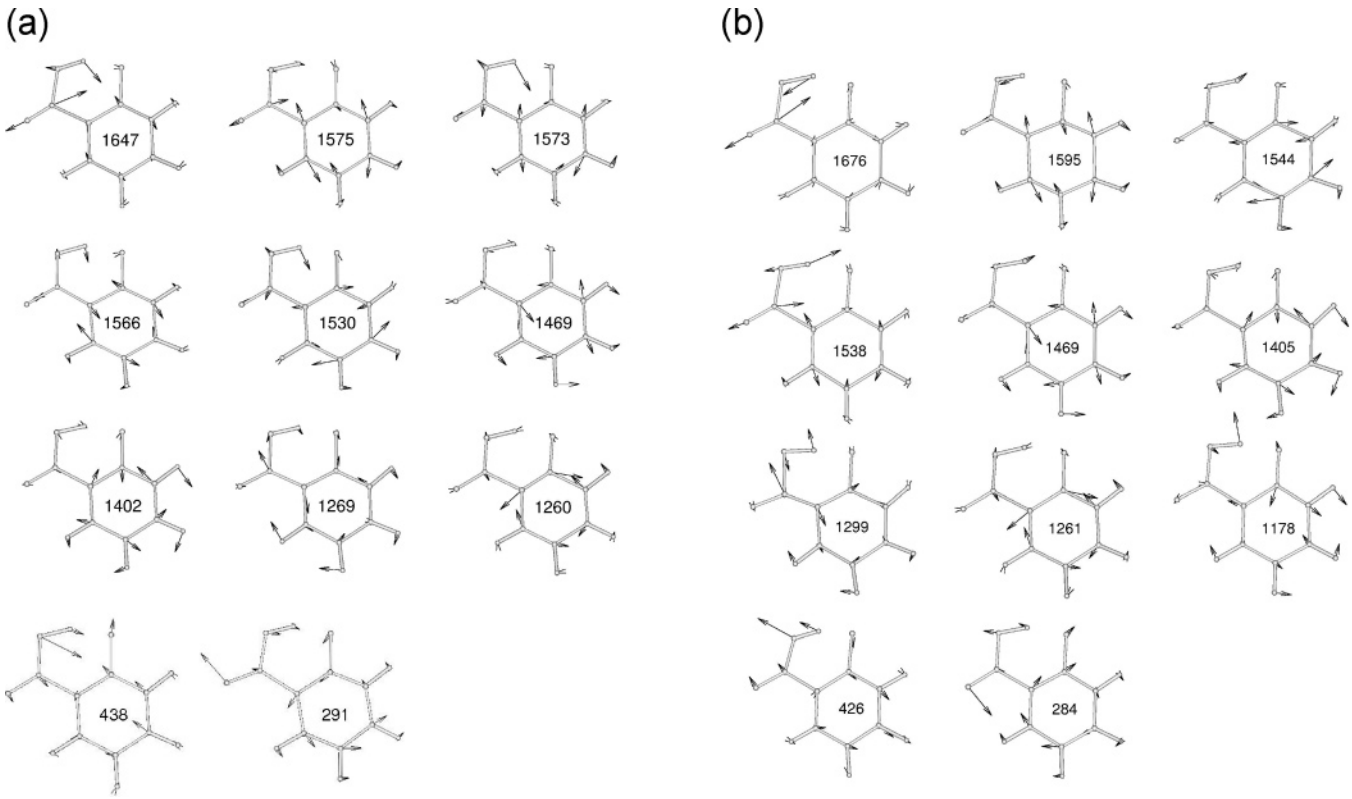

Figure 7. Selected normal modes of α-picolinic acid N-oxide ((a) undeuterated; (b) deuterated) calculated by the CPMD program in the harmonic approximation (frequencies (in cm^{-1}) inside of rings).

between 1647 cm^{-1} and 1469 cm^{-1} do not show the participation of the OH_s motion such as revealed by the NCA.[23] The too high frequency of 2158 cm^{-1} calculated for an OH_s-to-C═O_s coupled mode results from the harmonic approximation that is inherent to the CPMD calculation. In this context, it is useful to note the 2D potential of Stare and Balint-Kurti that includes periodicity and results in an almost perfect mixing of the COH_{be} and OH_s motions.[48] The calculated higher frequency mode of the pair is 1767 cm^{-1} (Table 2).

The CPMD calculation predicts four normal modes of the molecule in the 1650 cm^{-1} to 1480 cm^{-1} segment; each molecular mode splits into two components in the α polymorph and four in *β*. They are directly observable as shoulders on some bands or can be made so by band fitting. The crystal splittings are between <1 cm^{-1} and 7 cm^{-1}. The mode calculated to 1647 cm^{-1} involves large C═O_s and COH_{be} components (Figure 7a). The latter may be connected with the disappearance of the band at 1628 cm^{-1} in the INS spectrum (Figure 6a). However, the participation of the C═O_s coordinate in this mode is unlikely in view of the experimental evidence for the bands at 1678 cm^{-1} and 1720 cm^{-1} in the IR and Raman spectra to be the main C═O_s modes. The compelling evidence is the effect of ^{18}O substitution in the C═O group that causes shifts to 1650 cm^{-1} and 1700 cm^{-1}, respectively (S2a). In contrast to this mass effect stands one of deuterium substitution that causes a strong blue shift of the C═O_s bands (Figure 4b). This is an unusual coupling effect considering the fact that the C═O group is not directly involved in the motions of hydrogen; it will be further elaborated within the series of PANO congeners[28] since the blue deuteration shift is present in all the examples examined.

Besides the blue shift of the C═O_s bands, deuteration removes the broad absorption in the segment between the former and the Evans transmission at 1480 cm^{-1} leaving over a strong band at 1610 cm^{-1}. The strong peak at 1560 cm^{-1} also seems to be removed by deuteration (Figure 4b), but its Raman counterpart remains unchanged (Figure 5b). Both modes are due to ring vibrations since they are ubiquitous in the spectra of 2-substituted pyridine *N*-oxides.[58] The different effect of deuteration on their intensities in the IR and Raman spectra indicates that the 1610 cm^{-1} feature is due to a (pure) ring mode unlike the one at 1650 cm^{-1} in the IR spectrum that has a COH_{be} component contributing to its dipole moment derivative. This interpretation is in agreement with the CPMD calculation of the nearly degenerate modes at 1575 and 1573 cm-1 (Figure 7a); the former has no protonic component contrasting the marked one in the latter. However, frequency changes on deuteration of those and other modes in this segment do not agree with the experimental spectra. This is attributed to the harmonic OH_s and OD_s frequency calculation that leads to the coupling of the latter coordinate with the ring motions (Figures 7a,b; S1b), thus producing inadequate mode compositions and frequencies.

Most remarkable is the effect of cooling on the shape of the IR absorption in this segment appearing in the α polymorph (Figure 4a). The quartet of peaks of similar height may be connected with the shoulders on the peak at 1613 cm^{-1} in the spectrum recorded at >200 K. However, the mechanism of the relative intensity changes is obscure. Notable is the difference between both polymorphs and the fact that no effect comparable to one observed with the α polymorph appears with any other member of the series of PANO congeners.[28]

The location of the broad absorption corresponds not only to the predictions of the various model calculations (Table 2; Figures 7a,b; S1a,b) but also to the presence of bands, assigned to modes with large COH_{be} participation that are present in the spectra of structurally related compounds. Two examples are 4-nitro picolinic acid *N*-oxide (1499 cm^{-1}, S2c) and hydrogen maleate.[59] Moreover, in the Raman spectrum of PANO appears

a weak and broad, deuteration sensitive feature centered at ~1600 cm^{-1} that is underlying the carbonyl and the ring bands at 1615 and 1560 cm^{-1} (Figures 5a,b, inset). The combined computational and experimental results support strongly the location of the COH_{be} mode in the 1600 cm^{-1} segment. The COH_{be} coordinate is coupled with $C{=}O_s$ and ring motions and very probably with OH_s. However, the origin of the width of the IR absorption removed by deuteration asks for explanation. A plausible one is to consider it as part of the continuum separated by the Evans transmission at 1480 cm^{-1}. This possibility will be discussed jointly with the continuum.

Next to be scrutinized is the region below the Evans transmission at 1480 cm^{-1} for hydronic modes predicted by the frequency calculation of Stare and Balint-Kurti.[48] According to this, a band originating in a mixed OH_s and COH_{be} mode should appear at ~1300 cm^{-1}. A hydronic feature with unusual properties is indeed observed at a somewhat higher frequency, i.e., 1410 cm^{-1}. At room temperature, this is an unresolved peak on the flank of the strong ring band at 1432 cm^{-1}. On cooling to 200 K, the peak gains gradually in intensity, becoming the tallest band in the spectrum; it splits up on further cooling. It is removed by deuteration leaving over an unresolved peak at 1411 cm^{-1} that is even smaller and sharper than the original one. Simultaneously appears a new, composite band peaking at 1352 cm^{-1}. The markedly different effect of cooling on the two features suggests a difference in their origins. For the origin of the band peaking at 1352 cm^{-1} the DFT calculation on the isolated molecule (S1a) offers an alternative explanation in terms of modes characteristic of H-bonded carboxylic groups.[60,61] Accordingly to this, the band may be assigned to a coupled $C{-}O_s$ and COD_{be} mode with ring participation; its intensity should be very high. The CPMD calculated vibrational modes are in fair agreement with this representation in that the ring mode at 1269 cm^{-1} in which the in-phase $C{-}O_s$ and $N{-}O_s$ participate moves to 1299 cm^{-1} by acquiring a significant COD_{be} component. This should contribute to intensity of the new mode found at 1352 cm^{-1}. The predicted change upon deuteration of the lower frequency modes are observable with the IR and INS bands at 1280 cm^{-1} and of several Raman bands (Figures 4b, 5a,b and 6a). A weaker band of predominantly COD_{be} character is predicted to appear at 1072 cm^{-1}, but it is not detectable in the IR spectra of PANO. However, deuteration shifts observed with several bands in the segment between 1370 and 1000 cm^{-1} of the IR and Raman spectra (Figures 4b, 5a,b) indicate that the COD_{be} coordinate is coupled to ring modes with $C{-}O_s$ and $N{-}O_s$ participation. This is in agreement with the CPMD calculation (see Figure 7b and S1b) and also explains the frequency changes around 1280 cm^{-1} observed in the INS spectra (Figure 6a).

The agreement between the frequencies obtained from the CPMD calculation and the band frequencies in both sorts of spectra (Figures 4a,b and 5a,b) is acceptable considering the high density of bands and the effects of Evans transmissions. A more detailed analysis of the IR and Raman spectra is possible by comparison with the other members of the PANO series.[28] For the presently set goals, it is sufficient to note that the spectral changes in the region 1430−1640 cm^{-1} due to the hydronic mass effect on the bending frequency are in agreement with the assignment of the features in the 1500−1650 cm^{-1} region to the coupled modes with major COH_{be} participation and the hint to the possible origin of the band at 1352 cm^{-1} in the IR spectrum of PANO-*d*.

The origin of the band at 1410 cm^{-1} is more enigmatic. A CPMD calculated crystal mode does assume almost this frequency, but it is a pure ring mode (Figure 7a). This suits only the small peak left over after deuteration. It is possible that an accidentally degenerate protonic mode overlaps the ring mode, but this does not explain its excessive temperature dependence. The latter is also difficult to bring to agreement with conjectures of intensity borrowing from the underlying protonic continuum by some sort of Fermi resonance, although the Raman active mode at 1396 cm^{-1} may act by cleaving off a sharp band out of the continuum. Note that neither corresponding band does appear in the spectra of some PANO congeners[28] nor does it appear in the INS spectrum thus hinting to its relation with the continuum in that the latter is not at all expressed in the INS spectrum.

The analysis of the spectra of PANO and its isotopomers did not permit so far proposing a distinct feature for the candidate for the OH_s mode or mixed mode with dominant participation of this coordinate. This contrasts the spectra and NCA of the matrix isolated compound or its solutions.[23,33] This is also true for the INS spectra that are well-known to usually produce distinct OH_s bands in the example with strong H-bonds, including the intramolecular ones, e.g., hydrogenmaleate.[59] The failure in identifying distinct candidate(s) for the OH_s mode suggests the consideration of the continuum.

The extended absorption also seems to be present in the INS spectrum of PANO-*h*. Moreover it is not apparent in PANO-*d*, thus suggesting a possible protonic origin. This conclusion is excluded by a comparison of the spectra calculated[36] with and without inclusion of overtones (Figure 6b), which indicates that the extended absorption in the INS spectra of PANO-*h* originates from overtones. Indeed, a CLIMAX calculation with included overtones produces a remarkable match to the experimental INS spectrum; the obvious difference in the intensity of the extended absorption in the spectra of both isotopomers requires further attention.

The infrared continua are common with strong H-bonds in solutions and solids.[24] In the example of PANO, the continuum extends apparently from beneath the carbonyl bands into the far-infrared region down to ~300 cm^{-1} (S2a,d). Unfortunately, a reliable quantitative characterization of the continuum and the changes which may have resulted from deuteration or temperature changes is not possible owing to the numerous superimposed peaks and Evans transmissions that are also affected by those changes. For the same reason the center of gravity of the continuum cannot be determined reliably. However, qualitative observations based on Evans transmissions reveal a decay of absorbance in the region below 1400 cm^{-1}, but no significant effect of deuteration is observable except for the part between the carbonyl bands and the strong Evans transmission at 1480 cm^{-1}. This fact clearly shows the difference in the modes involved in the creation of the higher and lower frequency parts of the continuum.

As much as the Evans transmissions are hindering the acquisition of quantitative IR intensity data, they are helpful as qualitative indications for the very existence of the continuum. This realization is of prime importance since PANO does not comply with the requirements for the appearance of continua according to the theoretical treatment of their origin elaborated by Zundel and co-workers.[24] Prerequisite for the appearance of continua are the anharmonic double minimum potential functions allowing for large amplitude proton motions and the high polarizability of such H-bonds. In this theory, chelate H-bonds were explicitely exempted from the creation of continua because of the electronic short-circuit due to the conjugation in the chelate ring. However, restrictions for the appearance of continua

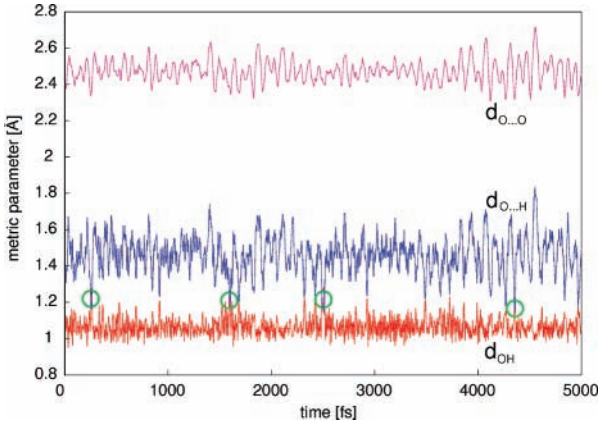

Figure 8. Dynamical CPMD profile of selected interatomic distances in α-picolinic acid *N*-oxide. Green circles denote cases where the proton is residing closer to the acceptor atom. Note that the displayed profiles refer to classical nuclear coordinates. See text for other details.

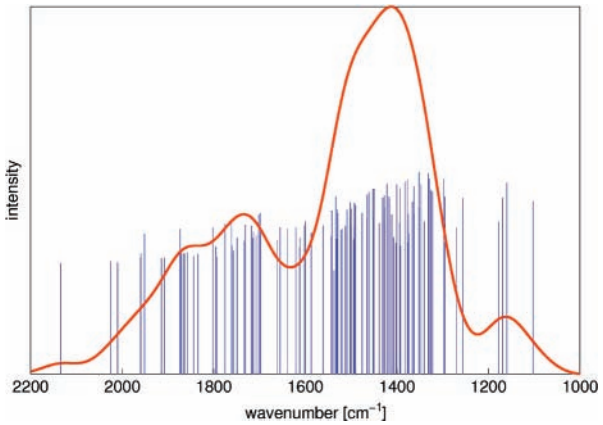

Figure 9. Distribution of anharmonic vibrational transitions (thin vertical lines) attributed to the OH stretching mode of α-picolinic acid *N*-oxide in the solid state, obtained from snapshots of the CPMD simulation, and the according envelope of the OH stretching band (curved line) assuming a Gaussian function of a constant half-width of 50 cm^{-1} for each individual transition.

postulated by Zundel and co-workers[62] are not met by the present example. Thus the diffraction results,[37] the potential functions calculated at any level for PANO and, particularly, the localization of the proton on one side of the H-bond according to the CPMD dynamics are in contradiction with the large amplitude proton motion as present in examples with double minima separated by low barriers that were treated by Zundel[24] and others. Moreover, conjugation in the chelate ring is present and thus the rise of a well-pronounced continuum in PANO and related compounds cannot be explained by theories based on large proton amplitude with concomitant large polarizability. We have therefore developed a novel approach that is not subject to the restrictions of such theory. Moreover, the novel approach also permits the prediction of the shape of the continuum contour with formation of absorption maxima.

CPMD Simulation of Crystalline α-PANO. The dynamical profile of d_{O-H}, $d_{O\cdots H}$ and $d_{O\cdots O}$ acquired from the CPMD simulation (Figure 8) shows that the hydrogen bond of PANO is essentially asymmetric. The proton is classically located about 99% of the simulation time closer to the donor oxygen atom ($d_{O-H} \leq d_{O\cdots H}$); the number of occasions with the proton transferred to the acceptor site are very rare, and structures with $d_{O-H} > d_{O\cdots H}$ do not appear to last for longer than a single large-amplitude O−H oscillation; no case has been observed where the proton would oscillate nearer to the acceptor oxygen. Apparently the hydrogen bond of PANO in the solid state does not exhibit much of a tendency for proton transfer and the time-averaged proton potential is of a single minimum type.

The extracted snapshot structures exhibit a notable diversity in geometry parameters, proton potentials and the pertinent anharmonic frequencies as expected. The dynamical profile of $d_{O\cdots O}$ covers a range between 2.294 and 2.718 Å. Variations in $d_{O\cdots O}$ affect the proton potential functions and thus the vibrational transition frequencies. Figure 2a shows some typical proton potentials acquired from snapshots of the dynamics and their corresponding $d_{O\cdots O}$. The potentials vary from a strongly asymmetric double-minimum type, consistent with large $d_{O\cdots O}$, to compressed (small $d_{O\cdots O}$) and somewhat asymmetric single minimum type. They are similar in shape to the ones calculated for isolated PANO molecules by static DFT calculations at different values of $d_{O\cdots O}$.[33] However, the proton potentials sampled from snapshots can be markedly different in shape even though the corresponding $d_{O\cdots O}$ are nearly the same (Figure 2a). Thus attempts to correlate the proton potential shape solely with $d_{O\cdots O}$ would probably not succeed because the fluctuating degrees of freedom other than the O···O distance do significantly influence the proton potential and the concomitant transition energies. In other words, indirect coupling to the OH_s mode is, besides by fluctuating $d_{O\cdots O}$, strongly influenced by other intra- and intermolecular degrees of freedom.

In line with the variation in proton potentials, the anharmonic OH_s frequencies are distributed over a wide range between 1100 and 2100 cm^{-1}. The frequency of each individual $0 \rightarrow 1$ vibrational transition is represented by a delta function whose height is proportional to the dipole-driven transition intensity in the approximation of electric harmonicity. Note that the differences in the calculated intensities originate solely from differences in the shapes of the anharmonic ground- and the first-excited-state wavefunctions as reflected in the various proton potentials acquired by the snapshots. The envelope of the transitions, displayed in Figure 9, was obtained by representing each individual transition as a Gaussian function of a half-width of 50 cm^{-1} centered at the pertinent frequency. Each of the Gaussians was scaled in such a way that its integral was equal to the calculated transition intensity.

The envelope of the density distribution exhibits a broad maximum at about 1400 cm^{-1} which could represent the OH_s mode in the spectrum. However, the coincidence in the positions of this maximum and the protonic band at 1410 cm^{-1} discussed in the previous section is most probably fortuitous. This conclusion is based on both the theoretical and experimental arguments. The frequencies appearing in the density distribution were obtained from one-dimensional potentials; we think that a realistic frequency simulation would require at least a five-dimensional hypersurface (OH_s, COH_{be}, C═O_s, C−O_s, N−O_s) in order to account for mode coupling. Nevertheless, it should be clear that the construction of a five-dimensional Born−Oppenheimer surface followed by solving the corresponding vibrational Schrödinger equation for several snapshots is not feasible in real time with the available computer power. In addition, the band maximum discussed above is not reliable from the experimental point of view, as it appears to be too narrow to be representative of a frequency distribution. It is much more probable that the rather broad maximum in the frequency distribution remains hidden by the distinct, strong bands and Evans transmissions. However, considering the weakness of the OH_s mode in comparable chelate compounds and the problem of locating the pertinent bands, indirect evidence for its expected location in the region around 1400 cm^{-1} can be taken from solution spectra[33] in which the absorption corresponding to a

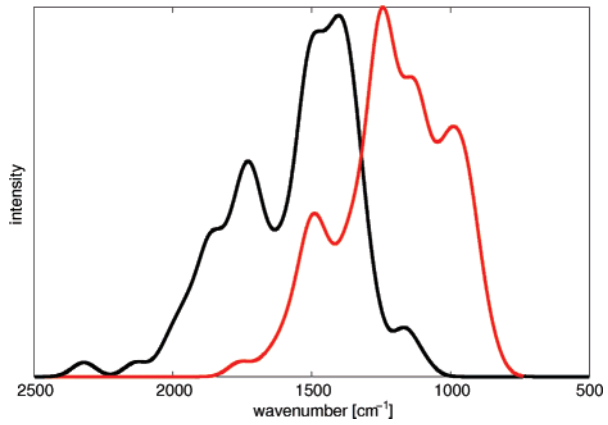

Figure 10. OH stretching (black) and OD stretching (red) envelope of solid-state picolinic acid *N*-oxide, calculated from snapshot potentials acquired by CPMD dynamics run (see text). Note that the intensity is scaled to equal peak values and does not reflect the mass effect.

mode with predominant OH_s character is more easily identifiable and found to be centered at about 1360 cm^{-1}.

The calculated envelope of the extended absorption corresponding to the hydrogen stretching motion of deuterated PANO-*d* is red-shifted with respect to one of the undeuterated species as expected. A comparison of OH_s and OD_s envelopes is shown in Figure 10. It is notable that the OD_s envelope has much the same width as that of OH_s and spans the interval between ~800 and ~1700 cm^{-1}. However, its shape is slightly different so that its maximum is at a frequency which is not much lower (~1250 cm^{-1}) than one of the OH_s envelope with the maximum at ~1400 cm^{-1}. This is roughly in accord with the observed IR spectrum of PANO-*d* that features a new band at 1352 cm^{-1}. It should be noted, however, that the envelopes of OH_s and OD_s transitions cannot be reliably compared between them because of the absence of information on their relative intensities. The OH_s absorption corresponding to the deuterated species is expected to have a lower integrated intensity than that of the undeuterated one, but no quantitative description of this aspect can be given. Further comparisons between the calculated stretching envelopes of PANO-*h* and PANO-*d* are thus not justified.

5. Concluding Remarks

For the interpretation of vibrational spectra of systems with strong H-bonds, it is imperative to collect as much as possible additional information on the physical characteristics of the H-bond, particularly ones related to the potential and its fluctuations. The data presented in the preamble of the Results and Discussion section form a fairly comprehensive set, but for the representation of H-bond dynamics and the interpretation of the spectra computational support is necessary. This regards in particular the outstanding features in the IR and INS spectra that are closely related to hydron motions. Perhaps more important than the band frequencies are their shapes as a source of information on the hydron dynamics. Among the internal coordinates describing the hydron motion it is the antisymmetric stretching that is of prime importance in this respect. However, due to the tendency of this motion to couple with other intra- or intermolecular motions it is necessary to include them in any type of theoretical treatments of band shapes and analyses of experimental spectra. Considering the short intramolecular H-bonds in crystalline PANO, the COH_{be} and crystal modes are the most important coupling partners. The latter replace the role of the intermolecular (slow) mode(s) in H-bonded dimers or other aggregates in the gas or liquid phases. Explicit anharmonic coupling of the OH_s motion with phonons has been elaborated previously.[63,64] Adjusted coupling parameters are needed in these theories whereas the effect of the crystal dynamics on the OH_s frequencies is included in the snapshot sampling of the system dynamics yielding a multitude of hydron potential functions from which the OH_s frequencies need to be extracted and complemented with transition probabilities. The calculation of the latter is the weak point of the treatment preventing the quantitative comparison of the integrated intensity area under the calculated contour with that of the experimental continuum. However, a reliable estimation of the latter is also not practical and therefore only the rough extent of the continuum and the position of the maxima in the calculated band contour are prone to comparison. Note that the frequencies were calculated from one-dimensional potentials and may therefore not correspond to the experimental ones. However, the IR spectrum of PANO-*h* does exhibit a protonic band at 1410 cm^{-1}, but its characteristics compared to OH_s absorptions observed with other examples of short intramolecular H-bonds, such as enolones, command caution in attributing to this mode before having understood the origin of those properties. This is also true of the band at 1352 cm^{-1} in the spectrum of PANO-*d*; its position fits the maximum in the distribution envelope calculated for this isotopomer (Figure 10). The alternative interpretation of the origin of this band (vide supra) should be added to the cautionary remarks made for the band at 1410 cm^{-1}.

The other maximum of the frequency distribution contour centered at about 1600 cm^{-1} coincides with the broad IR absorption and weak features in the Raman and INS spectra attributed to a protonic mode with dominant COH_{be}. This is adding weight to that attribution and to the evidence for the participation of the OH_s motion in the mode predicted by the 2D-potential calculation.[48] Notwithstanding the cautionary remarks, the combined evidence from the previous OH_s and COH_{be} frequency calculations as well as the novel CPMD-based approach suggest the attribution of the continuum to the mixed stretching and in-plane bending hydronic motions; the latter are likely to be more strongly engaged in the higher frequency part of the continuum. From the methodological point of view it is straightforward to extend the present approach to more dimensions, thus taking care of the couplings. However, this requires extremely large computational power. The empirical analysis of spectra would gain by dichroism studies of single crystals. Unfortunately, growing of appropriate crystals did not succeed. Single-crystal studies would also be of particular value in clarifying the problems raised by this work, particularly the origin of the band at 1410 cm^{-1} and the possible interactions between the hydron dynamics and intensities of ring modes predicting the unusual intensity behavior.

The molecular dynamics part of the present simulation gives a firm answer to the hydron motion between the two oxygens in that making unlikely the large amplitude motions, such as pertaining to a double minimum with a low barrier. Consequently, motions engendering high hydron polarizability do not seem to be involved in the creation of the continuum.

In addition to offering computational support to vibrational spectroscopy, the present method is also applicable to assist the interpretation of kinetic isotope studies in catalytic systems such as enzymes. The thermally averaged squared vibrational eigenfunctions have the meaning of a probability density, and the latter quantity is directly related to the potential of mean force.

Acknowledgment. Financial support of the Slovenian Ministry of Science, Higher Education and Technology (Grants

P1-0012 and P1-0010) is gratefully acknowledged. This work has also benefited from the use of facilities at the Center of Non-Linear Studies at Theory Division and the Lujan Neutron Scattering Center at LANSCE, which are funded by the Department of Energy's Office of Basic Energy Sciences. Los Alamos National Laboratory is operated by Los Alamos National Security LLC under DOE Contract DE AC52-06NA25396. We are grateful to Prof. Stewart Parker for collecting the INS spectra on the TOSCA spectrometer at the ISIS facility and to Prof. Boris Šket (Faculty of Chemistry and Chemical Technology, University of Ljubljana) for the synthesis of ^{18}O labeled PANO. Prof. W. B. Person and Dr. K. Szczepaniak (Gainesville), Prof. Savo Bratos (Paris), Prof. Mikhail Vener (Moscow), and Dr. Igor Reva (Coimbra) are thanked for critical reading of the manuscript. Warm thanks are due to Ms. Silva Zagorc for preparing the polymorphs and recording of the IR and Raman spectra. This work is dedicated to Foil A. Miller, a pioneer in classical infrared spectroscopy, on the occasion of his 90th birthday.

Supporting Information Available: Complete ref 41. S1. (a) Gas phase *Gaussian 03* B3LYP/6-31+G(d,p) harmonic frequency output for PANO-h and PANO-d (included in two separate files); (b) periodic CPMD BLYP/PW harmonic frequency output (written in the *Gaussian* format) for PANO-h and PANO-d (included in two separate files). S2a. Far IR spectra (polyethylene pellets) of crystalline picolinic *N*-oxide in protic and deuterated form. S2b. Infrared spectra of C=^{18}O isotopomer of solid-state picolinic acid *N*-oxide in KBr pellets. S2c. Infrared spectra of 4-nitropicolinic acid *N*-oxide in KBr pellets. S2d. A band decomposition of the IR spectrum of crystalline picolinic acid *N*-oxide. This material is available free of charge via the Internet at http://pubs.acs.org.

References and Notes

(1) Došlić, N.; Kühn, O. *Z. Phys. Chem.* **2003**, *217*, 1507.
(2) Wolf, K.; Mikenda, W.; Nusterer, E.; Schwarz, K.; Ulbricht, C. *Chem. Eur. J.* **1998**, *4*, 1418.
(3) Hayashi, T.; Mukamel, S. *J. Phys. Chem. A* **2003**, *107*, 9113.
(4) Barone, V.; Adamo, C. *J. Chem. Phys.* **1996**, *10*, 11007.
(5) Matanović, I.; Došlić, N. *J. Phys. Chem. A* **2005**, *109*, 4185.
(6) Alparone, A.; Millefiori, S. *Chem. Phys.* **2003**, *290*, 15.
(7) Krokidis, X.; Goncalves, V.; Savin, A.; Silvi, B. *J. Phys. Chem. A* **1998**, *102*, 5065.
(8) Mavri, J.; Grdadolnik, J. *J. Phys. Chem. A* **2001**, *105*, 2039.
(9) Mavri, J.; Grdadolnik, J. *J. Phys. Chem. A* **2001**, *105*, 2045.
(10) Tautermann, C. S.; Voegele, A. F.; Loerting, T.; Liedl, K. R. *J. Chem. Phys.* **2002**, *117*, 1962.
(11) Tayyari, S. F.; Emampour, J. S.; Vakili, M.; Nekoei, A. R.; Eshghi, H.; Salemi, S.; Hassanpour, M. *J. Mol. Struct.* **2006**, *794*, 204.
(12) Kovács, A.; Izvekov, V.; Zauer, K.; Ohta, K. *J. Phys. Chem. A* **2001**, *105*, 5000.
(13) Paul, S. O.; Schutte, C. J. H.; Hendra, P. J. *Spectrochim. Acta A* **1990**, *46*, 323.
(14) Tayyari, S. F.; Zeegers-Huyskens, T.; Wood, J. L. *Spectrochim. Acta A* **1979**, *35*, 1265.
(15) Bertolasi, V.; Gilli, P.; Ferretti, V.; Gilli, G. *J. Am. Chem. Soc.* **1991**, *113*, 4917.
(16) Emsley, J.; Ma, L. Y. Y.; Karaulov, S. A.; Motevalli, M.; Hursthouse, M. B. *J. Mol. Struct.* **1990**, *216*, 143.
(17) Emsley, J.; Ma, L. Y. Y.; Hursthouse, M. B.; Bates, P. A. *J. Chem. Soc., Perkin Trans.* **1989**, *2*, 527.
(18) Ilczyszyn, M. M.; Baran, J.; Ratajczak, H.; Barnes, A. J. *J. Mol. Struct.* **1992**, *270*, 499.
(19) Avbelj, F.; Hodošček, M.; Hadži, D. *Spectrochim. Acta A* **1985**, *41*, 89.
(20) Sandorfy, C. *J. Mol. Struct.* **2006**, *790*, 50.
(21) Tayyari, S. F.; Milani-Nejad, F. *Spectrochim. Acta A* **1998**, *54*, 255.
(22) Tayyari, S. F; Zahedi-Tabrizi, M; Laleh, S.; Moosavi-Tekyeh, Z.; Rahemi, H.; Wang, Y. A. *J. Mol. Struct.* **2007**, *827*, 176.
(23) Szczepaniak, K.; Person, W. B.; Hadži, D. *J. Phys. Chem. A* **2005**, *109*, 6710.
(24) Zundel, G. *Adv. Chem. Phys.* **2000**, *111*, 1.
(25) Kondratyuk, P. *Spectrochim. Acta A* **2005**, *61*, 589.
(26) Henri-Rousseau, O.; Blaise, P. *Adv. Chem. Phys.* **1998**, *103*, 1.
(27) We propose this term to designate the modes with large amplitudes of the acidic proton or deuteron displacements or percent in the potential energy distribution because the $OH(D)_s$ and $COH(D)_{be}$ internal coordinates participate in several normal modes.
(28) Stare, J.; Grdadolnik, J.; Hadži, D. Unpublished work.
(29) Szafran, M. *Bull. Acad. Pol. Sci.* **1965**, *13*, 245.
(30) Dziembowska, T.; Szafran, M. *Rocz. Chem.* **1974**, *48*, 1687.
(31) Brzeziński, B.; Zundel, G. *J. Phys. Chem.* **1982**, *86*, 5133.
(32) Dega-Szafran, Z.; Grundwald-Wyspiańska, M.; Szafran, M. *J. Mol. Struct.* **1992**, *275*, 159.
(33) Stare, J.; Mavri, J.; Ambrožič, G.; Hadži, D. *J. Mol. Struct. (THEOCHEM)* **2000**, *500*, 429.
(34) Panek, J.; Stare, J.; Hadži, D. *J. Phys. Chem. A* **2004**, 7417.
(35) Kearley, G. J. *J. Chem. Soc., Faraday Trans. 2* **1986**, *82*, 41.
(36) Kearley, G. J. *Nucl. Instrum. Methods A* **1995**, *354*, 53.
(37) Steiner, T.; Schreurs, A. M. M.; Lutz, M.; Kroon, J. *Acta Crystallogr. C* **2000**, *56*, 577.
(38) Car, R.; Parrinello, M. *Phys. Rev. Lett.* **1985**, *55*, 2471.
(39) Hutter, J.; et al. *Car-Parrinello Molecular Dynamics*, v. 3.7; IBM Zurich Research Laboratory: Zürich, Switzerland, 1995−2006.
(40) Hartwigsen, C.; Goedecker, S.; Hutter, J. *Phys. Rev. B* **1998**, *58*, 3641.
(41) Frisch, M. J.; et al. *Gaussian 03*, revision B.03; Gaussian, Inc.: Pittsburgh, PA, 2003.
(42) Clabo, D. A.; Allen, W. D.; Remington, R. B.; Yamaguchi, Y.; Schaefer, H. F., III. *Chem. Phys*. **1988**, *123*, 187.
(43) Nosé, S. *J. Chem. Phys.* **1984**, *81*, 511.
(44) Nosé, S. *Mol. Phys.* **1984**, *52*, 255.
(45) Hoover, W. G. *Phys. Rev. A* **1985**, *31*, 1695.
(46) Marston, C. C.; Balint-Kurti, G. G. *J. Chem. Phys.* **1989**, *91*, 3571.
(47) Balint-Kurti, G. G.; Dixon, R. N.; Marston, C. C. *Int. Rev. Phys. Chem.* **1992**, *11*, 317.
(48) Stare, J.; Balint-Kurti, G. G. *J. Phys. Chem. A* **2003**, *107*, 7204.
(49) Jezierska, A.; Panek, J.; Koll, A.; Mavri, J. *J. Chem. Phys.* **2007**, *126*, 205101.
(50) Jezierska, A.; Panek, J.; Borštnik, U.; Mavri, J.; Janežič, D. *J. Phys. Chem. A* **2007**, *111*, 5243.
(51) Meden, A.; Stare, J.; Hadži, D. Unpublished work.
(52) Tomasi, J.; Mennucci, B.; Cammi, R. *Chem. Rev.* **2005**, *105*, 2999.
(53) Stare, J.; Mavri, J. *Comput. Phys. Commun.* **2002**, *143*, 222.
(54) Mali, G.; Hadži, D. Unpublished work.
(55) Stare, J. *Dynamics and structure of systems containing short hydrogen bonds*; Ph.D. Thesis (in Slovenian); University of Ljubljana, 2003.
(56) Petterson, M.; Lundell, J.; Khriachtchev, L.; Räsänen, M. *J. Am. Chem. Soc.* **1997**, *119*, 11715.
(57) see Maréchal, Y. *The Hydrogen Bond and the Water Molecule*; Elsevier: Oxford, 2007 and references cited therein.
(58) Katritzky, A. R.; Hands, A. R. *J. Chem. Soc.* **1958**, 2195.
(59) Fillaux, F.; Leygue, N.; Tomkinson, J.; Cousson, A.; Paulus, W. *Chem. Phys.* **1999**, *244*, 387.
(60) Hadži, D.; Sheppard, N. *Proc. R. Soc. London A* **1953**, *216*, 247.
(61) See electronic supporting information of Burneau, A.; Génin, F.; Quilès, F. *Phys. Chem. Chem. Phys.* **2000**, *2*, 5020 (paper B006230H).
(62) Brzeziński, B.; Zundel, G. *Chem. Phys. Lett.* **1980**, *75*, 500.
(63) Fischer, S. F.; Hofacker, G. L.; Ratner, M. A. *J. Chem. Phys.* **1970**, *52*, 1934.
(64) Yaremko, A. M.; Ostrovskii, D. I.; Ratajczak, H.; Silvi, B. *J. Mol. Struct.* **1999**, *483*, 665.